

Unusual doping dependence of superconductivity in  $\text{Na}_y\text{FeAs}$ K. Sasmal,<sup>1</sup> B. Lv,<sup>2</sup> Z. J. Tang,<sup>2</sup> F. Chen,<sup>1</sup> Y. Y. Xue,<sup>1</sup> B. Lorenz,<sup>1</sup> A. M. Guloy,<sup>2</sup> and C. W. Chu<sup>1,3,4</sup><sup>1</sup>*Department of Physics and TCSUH, University of Houston, Houston, Texas 77204-5002, USA*<sup>2</sup>*Department of Chemistry and TCSUH, University of Houston, Houston, Texas 77204-5003, USA*<sup>3</sup>*Lawrence Berkeley National Laboratory, 1 Cyclotron Road, Berkeley, California 94720, USA*<sup>4</sup>*Hong Kong University of Science and Technology, Hong Kong, China*

(Received 2 March 2009; revised manuscript received 14 April 2009; published 18 May 2009)

Superconductivity and phase relationships were explored in the Na-Fe-As system. The PbFCl-type 111 phase is stable only within a Na stoichiometry range of 1.00 to  $\sim 0.85$ , and exhibits bulk superconductivity within an even narrower range around 0.90 in  $\text{Na}_{0.9}\text{FeAs}$ . In particular, stoichiometric NaFeAs is not a bulk superconductor. The onset of the superconducting transition varies in a totally different way and the highest  $T_c$  occurs in multiphase samples with a nominal composition of Na:Fe:As=0.5:1:1, where the superconductive volume-fraction is almost zero. Such doping dependency is rather surprising and in disagreement with most expectations.

DOI: [10.1103/PhysRevB.79.184516](https://doi.org/10.1103/PhysRevB.79.184516)

PACS number(s): 74.70.Dd, 74.62.Dh, 74.62.Bf

The recent discovery of superconductivity in layered transition-metal oxypnictides,  $\text{La}(O,F)\text{FeAs}$ ,<sup>1</sup> has attracted intense interest in the FeAs-based compounds. Superconductivity up to 55 K has been observed in three classes of FeAs-based compounds, i.e.,  $(R,Ae)(O,F)\text{FeAs}$ ,  $(Ae,A)\text{Fe}_2\text{As}_2$  and  $A\text{FeAs}$ , where  $R$ ,  $Ae$ , and  $A$  are rare earth, alkaline earth, and alkali elements, respectively.<sup>2-7</sup> The FeAs-based superconducting compounds have often been compared with the well-investigated cuprate superconductors. The doping dependency of the superconductivity, however, appears to be rather different in the FeAs-family as it varies significantly from one member to another.<sup>7,8</sup> The main doping effects reported so far in the FeAs family, however, appear still to be a smooth, bell-like  $T_c$  vs. carrier filling  $x_0$ , where  $T_c$  is the transition temperature. Competitions with magnetic ordering are often suggested in interpreting the data.<sup>9,10</sup> Significant change in the superconducting volume-fraction  $V_S$ , on the other hand, occurs only near the normal conductor-superconductor boundary. The  $V_S$ , it should be pointed out, is actually a convolution of the  $T_c(x_0)$  and the local  $x_0$ -distribution (composition inhomogeneity) if  $x_0$  is a sole parameter. A constant  $V_S$ , therefore, is expected if the superconductive range,  $\Delta$ , is much broader than the  $x_0$ -spread, e.g., the full width at half height (FWHM)  $\sigma$  of a normal distribution. The effect on  $T_c$ , in such cases, will be the main focus. At the opposite extreme of  $\Delta \ll \sigma$ , however, the spread would lead to the same  $T_c$  distribution but a drastic  $V_S$  change with  $x_0$ , though this is rarely observed or discussed. Herein we report our observations in the superconducting system,  $\text{Na}_y\text{FeAs}$ , which possesses a PbFCl-type structure isotopic to that of  $\text{LiFeAs}$ . This PbFCl-type structure as well as (trace) superconductivity exist over the whole nominal-composition range investigated, i.e., with the nominal composition of  $\text{Na}_y\text{FeAs}$ , with  $0.5 \leq y \leq 1.0$ . The samples are single phase, however, only for  $y \geq 0.9$ , and the impurity phase FeAs appears at lower  $y$ . A rather unusual doping effect is also observed. On one hand, the samples become bulk superconducting, e.g., with  $V_S > 10\%$ , only around  $y=0.9$  with an estimated spread  $\ll 0.1$ . The apparent  $T_c$ , on the other hand, monotonically increases with decreasing values of  $y$ . The  $T_c$  approaches its maximum where the  $V_S$  drops to zero.

This is different from what is expected for both  $\Delta \ll \sigma$  and  $\Delta \gg \sigma$ , and is difficult to understand. It seems that while the Na stoichiometry determines the superconducting range, the  $T_c$  onset is dominated by different factors. Candidates, for example, may be local defects/lattice distortion, which is expected to be more severe at lower  $y$ .

The polycrystalline samples were synthesized from high-temperature reactions of high-purity Na (ingot, 99.95%), Fe (pieces, 99.99%), and As (lumps, 99.999%). X-ray phase pure samples of FeAs powder were first prepared from the reaction of pure elements in sealed quartz containers at 600–800 °C. The ternary Na-Fe-As samples were prepared from solid-state reactions of high-purity Na with FeAs. Stoichiometric amounts of the starting materials with composition  $\text{Na}_y\text{FeAs}$  were placed and sealed in Nb tubes under Ar. The welded Nb tubes were then placed inside quartz tubes, evacuated and sealed, heated to 750 °C at a rate of 5 °C/min, and kept for 3 days before slowly cooled to 300 °C. Postannealing of the samples, between 300–400 °C, both within and without the Ar-filled Nb tubes, under continuous vacuum, were also carried out for representative samples. The polycrystalline samples so obtained are extremely sensitive to air. All manipulation and preparative steps were carried out within a purified Ar-atmosphere glovebox, with total  $\text{O}_2$  and  $\text{H}_2\text{O}$  level  $< 0.1$  ppm. Powder x-ray diffraction (XRD) analysis was performed using a Panalytical X'pert diffractometer, using copper radiation. Single-crystal x-ray analysis was also carried out on selected single crystals using a Siemens SMART diffractometer equipped with a charge-coupled device (CCD) area detector. Magnetization measurements were performed in a Quantum Design superconducting quantum interference device (SQUID) magnetometer. The four-lead resistance,  $R$ , was measured using a Quantum Design physical property measurement system (PPMS). The thermoelectric power,  $S$ , was measured using a homemade system. Precautions were taken to avoid any possible air contamination. Samples used in magnetization measurements were sealed either in thin quartz tubes or vacuum-grease coated gel-caps before being taken out of the glovebox.

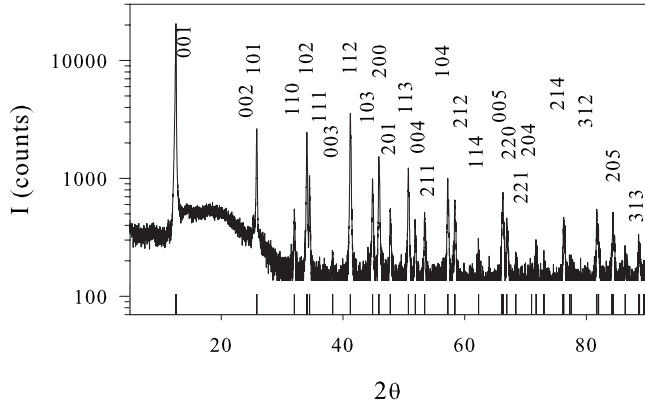


FIG. 1. The powder XRD of a  $y=1.0$  sample. The vertical bars at the bottom are the line positions of the  $P4/nmm$  cell.

The x-ray diffraction data from a single crystal ( $0.08 \times 0.06 \times 0.4$  mm<sup>3</sup>) with stoichiometric composition NaFeAs was investigated using the Siemens SHELXTL programs package. All 555 reflections can be attributed to an orthorhombic cell (spacegroup,  $P4/nmm$ ) with  $a=3.9866(16)$  Å and  $c=7.094(4)$  Å. The structural solution of NaFeAs follows that of LiFeAs.<sup>7</sup> Both Na and As atoms occupy the  $2c$  sites with the fractional  $z$  coordinates of 0.8542(4) and 0.2975(1), respectively. The resulting stoichiometric composition, Na<sub>1.0</sub>FeAs, was further confirmed by chemical analyses using inductively coupled plasma/mass spectrometer (ICPMS). The polycrystalline powder samples with varying nominal compositions were characterized using x-ray powder diffraction. The “Na<sub>y</sub>FeAs” samples are single phase for  $y=1.0$  and 0.9 based on XRD (Fig. 1). Noticeable impurity phase FeAs begins to appear at nominal compositions with  $y < 0.9$ , although the PbFCl-type Na<sub>y</sub>FeAs is still the main phase down to  $y=0.5$ . Analyses of the resulting lattice parameters of Na<sub>y</sub>FeAs and phase composition analyses (phase rule) results in an estimated compositional range of Na<sub>y</sub>FeAs, with  $y=1.00-0.85$ . Thermal annealing under dynamic vacuum at 300–400 °C of the as-synthesized Na<sub>y</sub>FeAs samples further indicates no compositional changes and that the phase width of Na<sub>y</sub>FeAs is insensitive to temperature. However, the situation at lower temperatures, e.g., around  $T_c$ , is less clear. The entropy associated with randomly distributed Na-vacancies, however, generally favors a smaller Na-content at lower temperatures, similar to the oxygen deficiencies in cuprates. The mixed-phase samples, in such a case, might even be metastable against a spontaneous decomposition below room temperature.

The samples were checked using a SQUID magnetometer under a field of 10 Oe. A small but noticeable magnetic background appears, which has the lowest value of  $4\pi\chi \approx 2 \cdot 10^{-3}$  for Na-compositions  $y \geq 0.90$ , and rises to 0.1 at either lower  $y$  or after air exposure. The magnetic background, fortunately, is only weakly dependent on the temperature between 20 and 50 K. The deduced  $4\pi(\chi - \chi_{30\text{ K}})$ , therefore, is used here (Fig. 2). The observed diamagnetic transitions are very broad. Both the zero-field-cooled susceptibility,  $\chi_{ZFC} - \chi_{ZFC,30\text{ K}}$ , and the field-cooled one,  $\chi_{FC} - \chi_{FC,30\text{ K}}$ , for example, vary with  $T$  almost linearly between 1.8 and 6 K for the  $y=0.9$  sample [Fig. 2(b)]. The diamag-

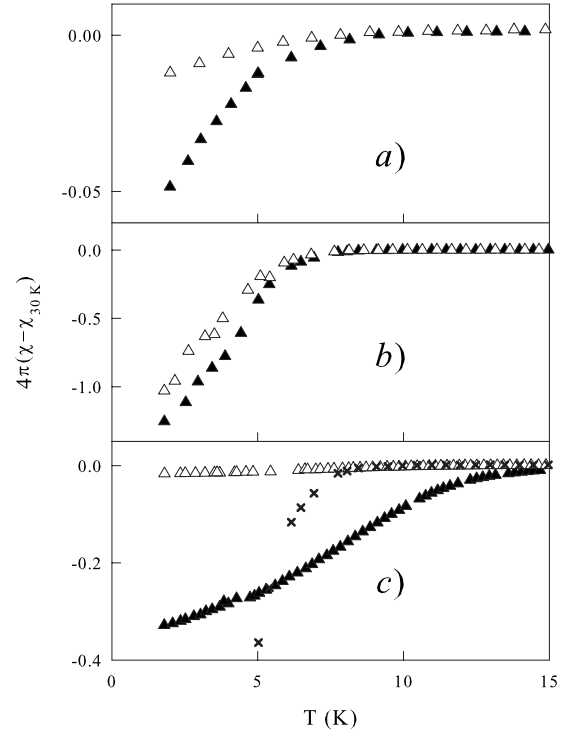


FIG. 2. The  $4\pi\chi_{ZFC}$  at zero-field-cooling (open triangles) and the field-cooling (solid triangles)  $4\pi\chi_{FC}$  at 10 Oe. (a):  $y=1.0$ ; (b)  $y=0.9$ ; and (c)  $y=0.5$ . The  $4\pi\chi_{ZFC}$  of the  $y=0.9$  sample (x's) is also plotted in Fig. 1(c).

netic  $4\pi(\chi_{ZFC} - \chi_{ZFC,30\text{ K}}) \approx 4\pi(\chi_{FC} - \chi_{FC,30\text{ K}})$ , however, persists far above this linear extrapolation, e.g., reaches  $-0.01$  at 8 K and still noticeable up to 9–10 K for the  $y=0.9$  sample. The split between  $\chi_{ZFC}$  and  $\chi_{FC}$  is even extended up to 50 K, and mixed with the magnetic hysteresis. The exact  $T_c$  onset, therefore, is difficult to determine. The intercept,  $T_{C0}$ , linearly extrapolated from the low- $T$  susceptibility, therefore, is used as the apparent  $T_c$  in the following discussion, with the understanding that trace superconductivity may even exist at much higher temperature due either to local defect-structures/Na-inhomogeneity or oxygen/H<sub>2</sub>O contaminations. It is interesting to note that the  $T_{C0}$  systematically increases with decreasing  $y$  (Fig. 2). The deduced  $T_{C0}$  are 6, 7, and 12 K, for example, for the  $y=1, 0.9$ , and 0.5 samples, respectively. To show this more clearly, the  $4\pi(\chi_{ZFC} - \chi_{ZFC,30\text{ K}})$  of the  $y=0.9$  sample is also shown in Fig. 2(c) and is significantly lower than that of the  $y=0.5$  sample above 7 K. The result, therefore, is also different from that expected for  $\Delta < \sigma$ .

It should be noted that the  $4\pi(\chi_{ZFC} - \chi_{ZFC,30\text{ K}}) \approx 4\pi(\chi_{FC} - \chi_{FC,30\text{ K}}) \approx -1.1$  at 2 K observed in the  $y=0.9$  sample is still lower than  $-1.5$  expected for a perfect superconducting sphere (or cube). A significant part of the sample might have even lower  $T_c$ . Such broad superconductive transitions seem to be a general characteristic of Na<sub>y</sub>FeAs. Previously reported data for  $y=1.0$  samples show similar behavior, where both the broad transition and the small  $|4\pi\chi_{ZFC,2\text{ K}}| \approx 0.1$  are in rough agreement with Fig. 1(a).<sup>11,12</sup> The samples, therefore, are inhomogeneous in terms of the superconductivity. Various low-temperature annealings, how-

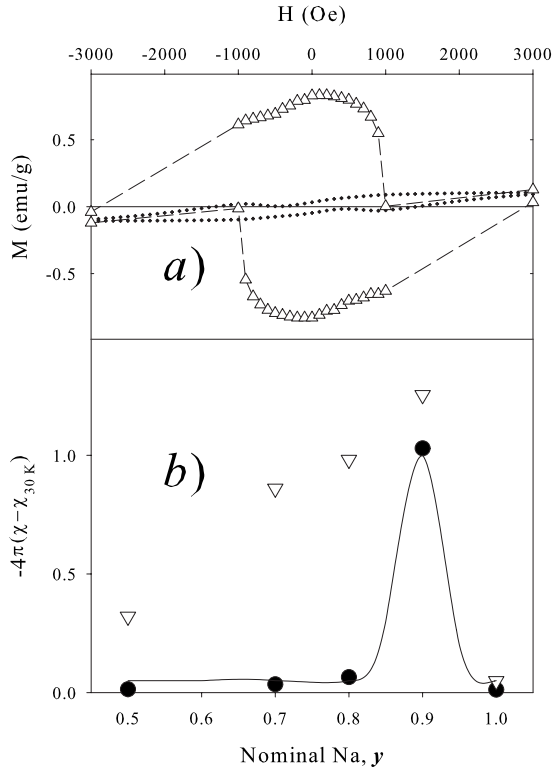


FIG. 3. a)  $M(1.8\text{ K})-M(25\text{ K})$  vs  $H$  for the  $x=0.9$  sample (open triangles) and the  $x=0.8$  sample (+'s). b) solid circles:  $-4\pi(\chi_{FC} - \chi_{FC,30\text{ K}})$ ; open triangles:  $-4\pi(\chi_{ZFC} - \chi_{ZFC,30\text{ K}})$ ; and the black line: the likely superconducting volume-fraction  $V_S$  (see text).

ever, have been tried without significant improvements. In particular, as will be discussed later, our data suggest that the Na migration is noticeable even at 200 K. Local Na inhomogeneity, therefore, should not be significantly worse than that associated with thermal fluctuations, at least not for some samples that were stored at room temperature for 2–3 months. The drastically different  $4\pi(\chi_{ZFC} - \chi_{ZFC,30\text{ K}})$ 's for the  $y=0.9$  and 1.0 samples further demonstrate that the spread  $\sigma$  is far less than 0.05 (Fig. 2). The broad transitions, therefore, demonstrate that either the doping range is extremely narrow or the  $T_c$ -spread is also affected by factors other than carrier filling.

A more drastic doping effect, however, appears to be the volume fraction (Figs. 2 and 3). The effect is obvious: both  $-4\pi(\chi_{ZFC} - \chi_{ZFC,30\text{ K}})$  and  $-4\pi(\chi_{FC} - \chi_{FC,30\text{ K}})$  drop from  $\approx 1.1$  at  $y=0.9$  to  $< 0.05$  at  $y=1.0$ . The data on stoichiometric NaFeAs single crystals further confirm that it is not a bulk superconductor. The situation for smaller  $y$  ( $< 0.9$ ), however, is rather vague with a big difference between the zero-field-cooled (ZFC) and field-cooled (FC) susceptibilities. While a lower  $-4\pi(\chi_{FC} - \chi_{FC,30\text{ K}})$  is often attributed to strong-flux pinning, an almost identical  $-4\pi(\chi_{ZFC} - \chi_{ZFC,30\text{ K}})$  and  $-4\pi(\chi_{FC} - \chi_{FC,30\text{ K}})$  in the similar  $y=0.9$  sample cast doubts. It is especially interesting to note that both  $-4\pi(\chi_{ZFC} - \chi_{ZFC,30\text{ K}})$  and  $-4\pi(\chi_{FC} - \chi_{FC,30\text{ K}})$  of the  $y < 0.9$  samples increase significantly after samples are exposed to air, sometimes by an order of magnitude. The as-synthesized samples were exposed to either humid air or kept in desiccated bottles with no significantly different results.

Enhancements of up to five- to tenfold were observed upon exposure of up to a few days. Similar enhancement has also been reported after  $\mu\text{SR}$  measurement (presumably with some unavoidable air exposure).<sup>12</sup> While the exact mechanism is not clear, the phenomena strongly suggest that the superconducting parts of the  $y < 0.9$  samples may be concentrated on the surfaces and that the samples might not even be superconductive in their neat states. To verify this, a procedure was developed to compare the relative  $V_S$  through the  $M$ - $H$  loops at 2 K. The  $M$ - $H$  loop of a type II superconductor is a superposition of a hysteretic part,  $M_{\text{irr}} \propto J_c d$  (the flux pinning), and a reversible part,  $M_{\text{rev}} \propto 1/\lambda^2$ , where  $J_c$ ,  $d$ , and  $\lambda$  are the critical current density, sample/grain size and penetration depth, respectively. Both should be proportional to  $V_S$  in phase-inhomogeneous samples if no drastic changes in  $J_c$ ,  $d$ , and  $\lambda$  are expected. As a further approximation, the average  $M_{\text{ave}}$  is used here as the estimation of  $M_{\text{rev}}$ .

To avoid the magnetic background,  $M(H)$  (1.8 K)- $M(H)$  (25 K) of the  $\pm 5\text{ T}$  loops of the  $y=0.9$  and  $y=0.8$  samples are shown in Fig. 3(a). The  $M(H)$ 's (25 K) of all samples are ferromagnetic like,  $< 0.1\text{ emu/g}$  below 5 T, with negligible hysteresis and insensitive to  $y$ , for  $y > 0.7$ . While the  $y=0.9$  sample shows a typical  $M$ - $H$  loop of a type II superconductor with the  $M_{\text{ave}}$  being diamagnetic on the order of a few  $\text{emu/cm}^3$ , the  $M_{\text{ave}}$  of the  $y=0.8$  sample is paramagnetic with the amplitude one order-of-magnitude smaller, apparently dominated by the residual background. The hysteretic split of the  $y=0.8$  sample is also tenfold smaller, excluding the possibility that the  $J_c d$  (flux pinning) of the  $y=0.8$  sample is much larger than that of the  $y=0.9$  sample. The  $V_S$  of the  $y=0.8$  sample, therefore, seems to be at least tenfold smaller than that of the  $y=0.9$  sample, and closer to the  $-4\pi(\chi_{FC} - \chi_{FC,30\text{ K}})$  value [the solid circles in Fig. 3(b)]. We therefore use the observed  $-4\pi(\chi_{FC} - \chi_{FC,30\text{ K}})$  to represent  $V_S$ . This estimated volume fraction appears as a  $\delta$  function of  $y$ . It should be noted that  $\text{Na}_y\text{FeAs}$  is still the dominant phase down to  $y=0.5$  based on the XRD observed. The disappearance of the superconductivity actually occurs within (but rather close to) the phase range limits. While such an extremely narrow doping range might be one of the reasons for the broad transition observed, the higher  $T_{c0}$  in the  $y=0.5$  sample presents a challenge (Fig. 2). It is hard to think that a single-value  $T_c(y)$  correlation can have the highest  $T_c$  located at an edge of doping range. This situation is certainly very different from that of the other FeAs-based superconductors. Factors other than the doping levels might be needed to understand the opposite effects on  $T_c$  and  $V_S$ . It might not be a mere coincidence that the  $\text{Na}_y\text{FeAs}$  phase at  $y < 0.9$  is near its substoichiometric-phase range limit. Dense lattice defects and/or distortions, therefore, are expected in  $y < 0.9$  samples. A larger  $T_c$  onset and a reduced  $V_S$  could simultaneously occur if the volume fraction were dominated by the undistorted part but the onset significantly enhanced in a minor distorted part.

The optical reflectivity and the apparent magneto resistance up to 50 K in a nearly stoichiometric NaFeAs single crystal has recently been reported as the evidence for possible spin density wave (SDW).<sup>13</sup> The resistance  $R(T, H)$  of the  $y=0.9$  sample, therefore, was measured to verify the possible competition between superconductivity and SDW (Fig.

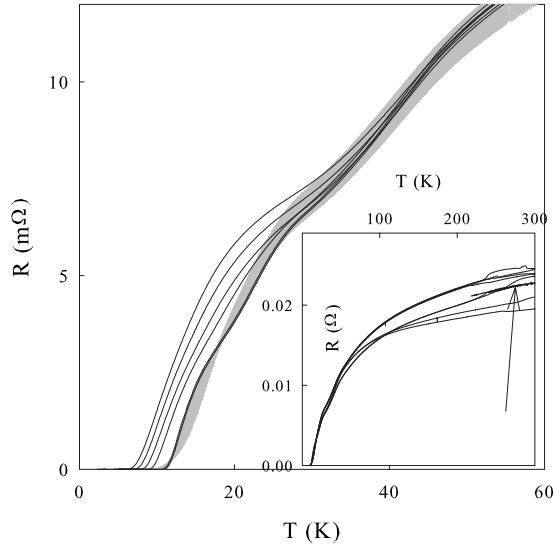


FIG. 4.  $R(T, H)$ 's of the  $y=0.9$  sample. The lines from left to right are at  $H=7, 3, 5, 1,$  and  $0$  T, respectively. The grey band is the estimated experimental uncertainty due to the shifts (see text). Inset: The zero-field resistance monitored over the measurement period. The irregular jumps (one of them is indicated by an arrow) between 230 and 300 K suggest the possible Na migration and the  $R$  shift associated.

4). The superconducting transition is clear with the zero-field resistance reaching zero at  $T_0=12$  K, which is higher than the  $T_{c0}$  deduced. Under fields, the zero-resistance temperature shifts to lower temperature as expected. The suppression rate of  $0.4$  K/T is comparable to, but slightly higher than, that of other FeAs-based superconductors, e.g.,  $0.25$  K/T for  $\text{Ba}_{0.6}\text{K}_{0.4}\text{Fe}_2\text{As}_2$ .<sup>14</sup> Together with the total flux expulsion (Meissner effect) presented above, the bulk superconductivity in the Na-deficient  $\text{Na}_{0.9}\text{FeAs}$  is demonstrated. The question of where the superconductivity onset is, however, again presents a challenge. The field-induced  $R$  splits persist up to  $40$  K or higher, roughly consistent with the splits between  $\chi_{\text{ZFC}}$  and  $\chi_{\text{FC}}$  observed. To explore the issue, additional zero-field resistance was repeatedly measured between  $5$  and  $300$  K for 4 days, both before and after the high-field measurements (inset, Fig. 4). It is interesting to note that the resistance occasionally jumped at  $200$  K or higher (shown as arrows), and that the  $R$  is irreversible after such jumps. Although the grain-boundary oxidation may cause such jumps, the less affected  $R(T)$  below  $50$  K suggests that the Na migration above  $200$  K may also be a factor. It is interesting to note that such a high-migration rate is also needed to interpret the above diamagnetic moment increase after exposure to air. Without a significant Na migration/re-arrangement on a depth-scale comparable with  $\lambda$ , a large increase in  $\chi_{\text{ZFC}}$  is difficult unless oxygen-contaminated Na-Fe-As were also superconducting with similar  $T_c$ . To estimate the field effects, all zero-field data during the 4-day measurements is marked as a grey band in Fig. 4, and regarded as the experimental uncertainty. The field effects below  $25$  K are clearly larger than the possible experimental uncertainty. The parallel shifts between  $12$  and  $25$  K, and the reasonable  $dT_0/dH$  value observed strongly suggest possible trace superconductivity far

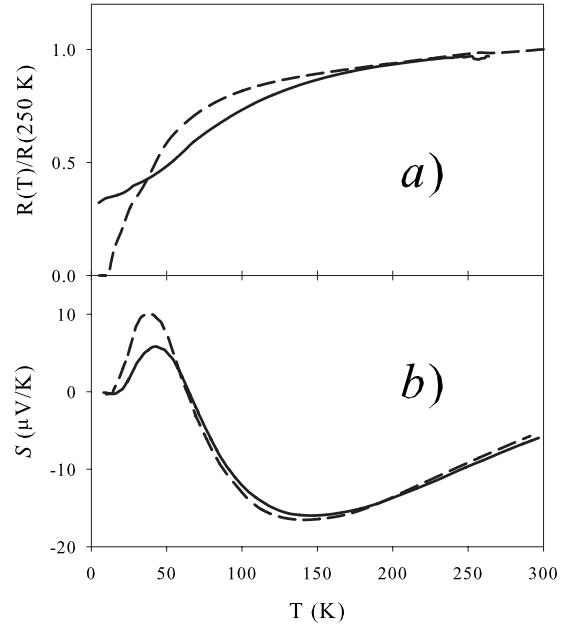


FIG. 5. (a) The zero-field resistance of Na-Fe-As samples with  $y=0.9$  (dashed line) and  $y=1.0$  (solid line). (b) Thermoelectric power of the  $y=1.0$  (solid line) and the  $y=0.9$  (dashed line) samples.

above  $20$  K. This temperature is almost three to four times that of the  $T_{c0}$  extrapolated but consistent with the observed diamagnetic drops far above  $T_{c0}$ . The effects at higher temperature, however, are less clear. The field effects are comparable with the 4-day drifts of the zero-field resistance, although a systematic up-shift with  $H$  is still clear and rather similar to the data of Ref. 12. It is interesting to note that the sample with its  $4\pi(\chi_{\text{FC}} - \chi_{\text{FC}, 30\text{ K}}) \approx -1.1$ , should not possess the positive magneto resistance associated with SDW. In particular, the same field effects between  $25$  and  $50$  K have also been observed in other samples with  $0.5 \leq y \leq 1$ . No indications of evolution from SDW to superconductivity can be seen in our data.

To further explore the issue, the  $R(T)$ s and the thermoelectric power  $S(T)$  at zero field for two samples with  $y=1.0$  and  $y=0.9$  are compared in Fig. 5. Despite the large residual  $R(T=2\text{ K})$  of the nonsuperconducting  $y=1.0$  sample, both have similar temperature dependency at high temperatures. Again, no indications of a SDW-to-superconductivity evolution, such as that in  $(R, \text{Ae})(O, F)\text{FeAs}$ ,<sup>15</sup> can be seen. The thermoelectric power,  $S$ , is also very similar for the two samples, although one is bulk superconductor and the other is not [Fig. 5(b)].

It should be noted that the disappearance of bulk superconductivity below  $y=0.8$ , is even more difficult to understand. If the competing magnetic order is the main factor, the SDW has to reappear at lower  $y$ . It is also hard to understand the observation that the maximum  $T_c$  is actually located outside such narrow bulk-superconductive range. Some other factors, therefore, may also contribute to the doping effect in the Na-Fe-As system. It is interesting to note that the superconductive properties of  $\text{LiFeAs}$  and  $\text{NaFeAs}$ , e.g., the



doping dependency and the transition sharpness, are rather different.<sup>16</sup> The differences between the ion size and the electronegativity may play a role.

In summary, superconductivity has been observed in the Na-Fe-As system within an extremely narrow range of the Na stoichiometry. Although the major diamagnetic transition occurs at a relatively low-temperature range of 7–12 K, the resistivity under field suggests a possible onset of 20 K or higher. The observations show that the superconductivity in this compound might not be dominated by the carrier concentration, and that other factors may also play important roles.

This work is supported in part by the T. L. L. Temple Foundation, the John J. and Rebecca Moores Endowment, the State of Texas through the Texas Center for Superconductivity, the U. S. Air Force Office of Scientific Research, and at Lawrence Berkeley Laboratory by the Director, Office of Science, Office of Basic Energy Sciences, Division of Materials Sciences and Engineering of the U.S. Department of Energy under Contract No. DE-AC03-76SF00098. A.M.G., Z.T. and B.L. acknowledge the support from the NSF (Grant No. CHE-0616805) and the Robert A. Welch Foundation.

- 
- <sup>1</sup>T. Watanabe, H. Yanagi, T. Kamiya, Y. Kamihara, H. Hiramatsu, M. Hirano, and H. Hosono, *Inorg. Chem.* **46**, 7719 (2007).
- <sup>2</sup>Z. A. Ren, W. Lu, J. Yang, W. Yi, X. L. Shen, Z. C. Li, G. C. Che, X. L. Dong, L. L. Sun, F. Zhou, and Z. X. Zhao, *Chin. Phys. Lett.* **25**, 2215 (2008).
- <sup>3</sup>C. Wang, L. Li, S. Chi, Z. Zhu, Z. Ren, Y. Li, Y. Wang, X. Lin, Y. Luo, S. Jiang, X. Xu, G. Cao, and Z. Xu, *EPL* **83**, 67006 (2008).
- <sup>4</sup>M. Rotter, M. Tegel, and D. Johrendt, *Phys. Rev. Lett.* **101**, 107006 (2008).
- <sup>5</sup>K. Sasmal, B. Lv, B. Lorenz, A. M. Guloy, F. Chen, Y.-Y. Xue, and C.-W. Chu, *Phys. Rev. Lett.* **101**, 107007 (2008).
- <sup>6</sup>X. C. Wang, Q. Q. Liu, Y. X. Lv, W. B. Gao, L. X. Yang, R. C. Yu, F. Y. Li, and C. Q. Jin, *Solid State Commun.* **148**, 538 (2008).
- <sup>7</sup>J. H. Tapp, Z. Tang, B. Lv, K. Sasmal, B. Lorenz, P. C. W. Chu, and A. M. Guloy, *Phys. Rev. B* **78**, 060505(R) (2008).
- <sup>8</sup>C. de la Cruz, Q. Huang, J. W. Lynn, J. Li, W. Ratcliff II, J. L. Zarestky, H. A. Mook, G. F. Chen, J. L. Luo, N. L. Wang, and P. Dai, *Nature (London)* **453**, 899 (2008).
- <sup>9</sup>I. A. Nekrasov, Z. V. Pchelkina, and M. V. Sadovskii, *JETP Lett.* **87**, 560 (2008).
- <sup>10</sup>D. J. Singh and M. H. Du, *Phys. Rev. Lett.* **100**, 237003 (2008).
- <sup>11</sup>D. R. Luhman, W. Pan, D. C. Tsui, L. N. Pfeiffer, K. W. Baldwin, and K. W. West, *Phys. Rev. Lett.* **101**, 266804 (2008).
- <sup>12</sup>D. R. Parker, M. J. Pitcher, P. J. Baker, I. Franke, T. Lancaster, S. J. Blundell, and S. J. Clarke, *Chem. Commun. (Cambridge)* (2009) 2189.
- <sup>13</sup>G. F. Chen, W. Z. Hu, J. L. Luo, and N. L. Wang, arXiv:0902.1100 (unpublished).
- <sup>14</sup>G. Mu, H. Q. Luo, Z. S. Wang, L. Shan, C. Ren, and H. H. Wen, *Phys. Rev. B* **79**, 174501 (2009).
- <sup>15</sup>J. Dong *et al.*, *EPL* **83**, 27006 (2008).
- <sup>16</sup>C. W. Chu, F. Chen, M. Gooch, A. M. Guloy, B. Lorenz, B. Lv, K. Sasmal, Z. J. Tang, J. H. Tapp, and Y. Y. Xue, *Physica C* (unpublished).